EquiSpaced Unshaded Line Array Method For Target Identification Using Side Scan Sonar Instrument

M Z Lubis[1*], S Irawan[1], W Anurogo[1], H Kausarian[2], S Pujiyati[3]

[1] Geomatics Engineering, Politeknik Negeri Batam, Batam 29461, Indonesia
[2] Faculty of Engineering, Universitas Islam Riau, Pekanbaru, 28284, Indonesia
[3] Department of Marine Science and Technology, Institut Pertanian Bogor, Indonesia

*Email: zainuddinlubis@polibatam.ac.id

Abstract. The Beam Pattern Discrete equispaced unshaded Line Array Method was used to compute the two-dimensional beam pattern which depends on the angle of the incoming sound waves from the axis of the array were accepted have been depending on the angle at which the sound beam array. This research was conducted in December 2016 in the Punggur Sea, Batam, Riau Islands-Indonesia, and its coordinate system is 104° 08.7102 E and 1° 03.2448 N until 1° 03.3977 N and 104° 08.8133 E, Discrete-Beam Equispaced unshaded Line Array method in target 4 has the highest value in the directivity pattern is 21.08 dB. The results of the beam pattern model show that neither the central value at the incidence angle (o) of the directivity pattern (dB) were not at the 0 (zero) or the beam pattern central have been generated by the target 6 with incident angle -1.5 o and 1.5o. In addition, it has declined by 40 dB. Highest result of line trace is target 1 with 191, 88 cm on target 1, and highest of time result is 13568 cm/second on target 4. Target 1 have a relationship with results with highest target detection of side scan sonar imagery. Seismic figure of side scan sonar imagery have total line trace is 4479, time: 77.9547 cm/s, and gain: 0.00271091.

Keywords: Side Scan Sonar, Punggur Sea, Beam Pattern, EquiSpaced Unshaded Line Array

1. Introduction

Punggur sea is the part of the Riau Islands in Indonesia. Generally Punggur sea still rarely done research on the identification of seabed using the acoustic wave technology. Worldwide, these marine environments have not been studied using high-resolution hydro-acoustic methods (eg, bathymetry, and base profiles), useful for investigation of sediment processes, benthic habitats, mineral resources, artificial artifacts, and other features. Side-scan sonar imagery and underwater photography, coupled with bathymetric and sedimentologic data, revealed noteworthy features and the interplay of multiple processes on the riau island and punggur sea, Indonesia. The seafloor imagery, target identification, and image processing with two dimensional was conducted on the punggur sea in 2017 [1-2].

The SSS is a sonar development that able to observe and show the two-dimensional surface pictures by the counter of the sea floor, topography, and the target simultaneously. This instrument is able to distinguish the small particles of the seabed structure such as rocks, muds, sand, gravel, or basic types other waters [3]. Side-scan sonar is an active sonar system which implemented the characteristics of sideways look, two channels, narrow beam, and towed body [4-5]. The passive

acoustic monitoring method with species-specific transmission beam pattern influences the facility with which animals can be localized by a hydrophone array [6].

The principle of a side scan sonar can be seen in Figure 1, and the system resolution: governed by the shape of the acoustic beam and the length of the transmitted pulse [7-8]. So it depends on the three-dimensional distribution of the acoustic energy of the system that affects the size of the footprint. If the side-scan sonar has low frequency sources (10-30 kHz), the sound pulse will be transmitted and received at long range (covering a large area in a short time) [9-10]. More particularly, the application of the system is wide-ranging in marine geology, marine biology, hydrography, underwater archaeology, oceanic engineering, and surveys for military purposes. Regarding the monitoring technologies of benthic artificial habitats, the side-scan sonar system has been proposed as the most practical [11-12]. However, due to the cost of the system, the complexities of its operation procedures, the necessities of a precise track chart for the ship, and extensive period of time and experience for data processing.

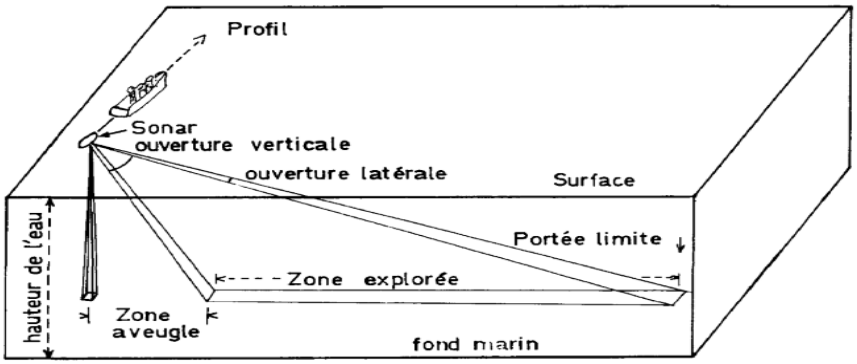

Figure 1. Principle of a side scan sonar

2. Methods

2.1. Study Area

This research was conducted in December 2016 at the Punggur Sea, Batam, Riau Islands, Indonesia at the coordinate of 104 ° 08.7102 E and 1 ° to 1 ° N 03.2448 03.3977 08.8133 N and 104 ° E . This research has 3 tracks (Figure 2). Acoustic data acquisition was done using a Side Scan C-Max CM2 sonar tow fish instrument and also it was set at a frequency of 325 kHz and with a maximum distance of 200 m and 25 m cable length, this study location can be seen in Figure 2.

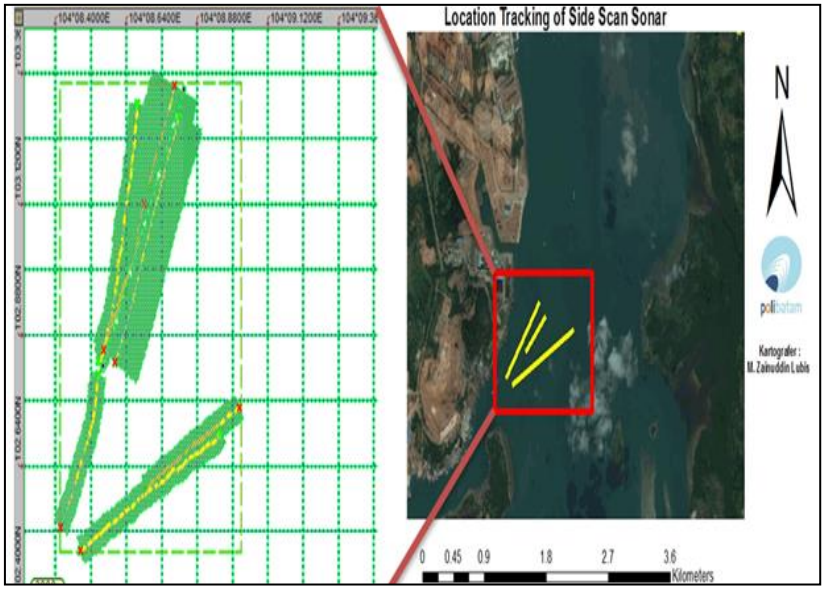

Figure 2. The location of the side scan sonar recording and its observation.

2.2. Two-Dimensional Beam Pattern

The characteristics of beam pattern C-Max CM2 Side Scan Sonar Tow fish can be seen in Figure 3.

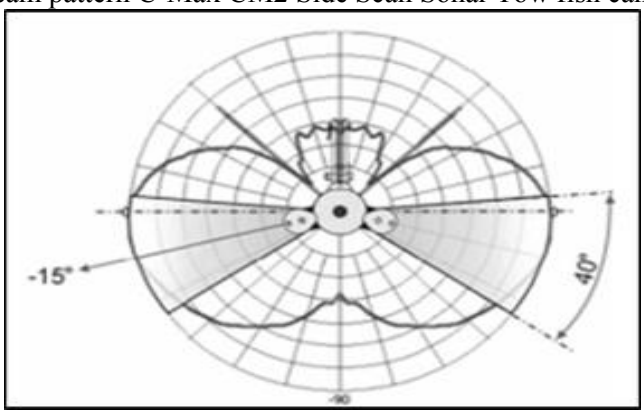

Figure 3. The beam pattern C-Max CM2 of the Side Scan Sonar Tow fish characteristic.

Calculating the two-dimensional beam pattern depends on the angle of the incoming sound waves from the array axis, the received power depends on the angle at which light sound incident to array. We can describe this angular dependence with an equation to relate the actual strength that was accepted for the average time power to the shaft (where, θ = 0° and the maximum power is a). The Beam Pattern Discrete-Equi-Spaced Unshaded Line Array can be seen in (Figure 4). This ratio is a function of beam pattern two-dimensional array, b (θ) where:

$$b(\theta)=\frac{\langle P(\theta)\rangle}{\langle P(\theta=0°)\rangle}=\frac{\frac{(Mp_{max})^2}{R}(1+\cos\delta)}{\frac{(Mp_{max})^2}{R}(1+\cos 0°)}$$

$$b(\theta)=\frac{\frac{(Mp_{max})^2}{R}(1+\cos(kd\sin\theta))}{2\frac{(Mp_{max})^2}{R}}=\frac{(1+\cos(kd\sin\theta))}{2} \quad (1)$$

Using a geometric identification in the sonar system:

$$1+\cos\theta=2\left(\cos^2\left(\frac{\theta}{2}\right)\right):$$

$$b(\theta)=\left[\cos^2\left(\frac{kd\sin\theta}{2}\right)\right]$$

or

$$b(\theta)=\left[\cos^2\left(\frac{\pi d\sin\theta}{\lambda}\right)\right] \quad (2)$$

$$b(\theta)=\left(\frac{V}{n}\right)^2=\left[\frac{\sin\left(\frac{n\pi d}{\lambda}\sin\theta\right)}{n\sin\left(\frac{\pi d}{\lambda}\sin\theta\right)}\right]^2 \quad (3)$$

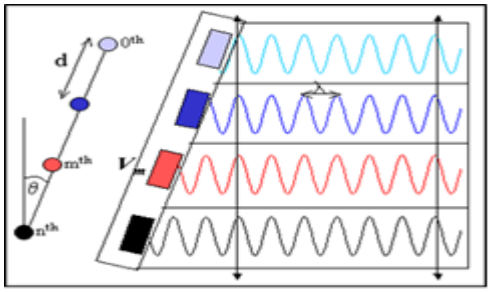

Figure 4. The Beam Pattern Discrete-Equi-Spaced Unshaded Line Array.

3. Results and discussion

Generally, the upper slope of the seafloor will be filled by fine grained sediments and the bottom will be filled by coarse grained sediments. It was caused by the gravity force. However, based on the side scan sonar image can be seen the differences between the texture and roughness clearly on the sediments of sand, biogenic sand and mud. There are 7 targets were detected by recording the image of Side Scan Sonar used C-MAX with an estimation of target detection could be observed the large object by the visual images on the target 6 at coordinates 1° 03.3977 N and 104° 08.8133 (Figure 5). These objects can be indicated was a sunken wreck on the seabed of Punggur sea, Batam, Riau Islands, Indonesia. The result of the time acquisition, ping position, gain and elevation of the SSS recording can be seen in Table 1. In addition, Figure 5 shows the image result of the seabed.

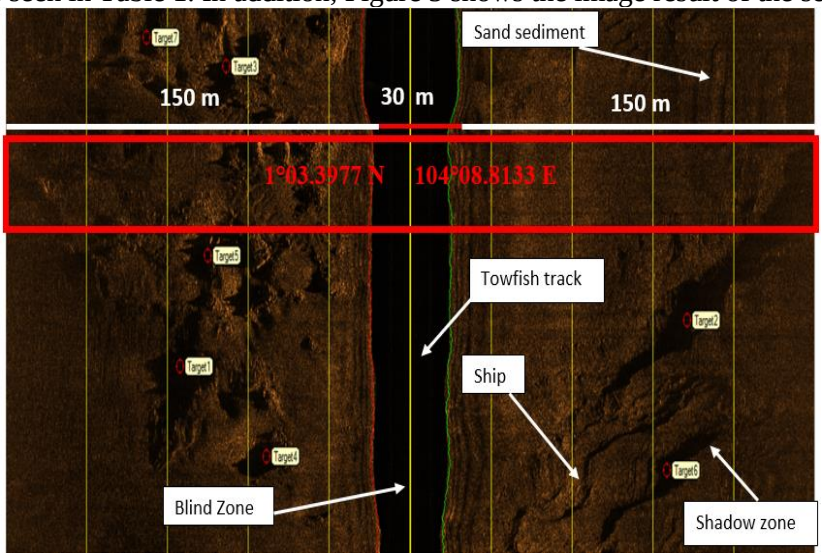

Figure 5. The classification of the seafloor sediments in the Punggur sea.

There are several lines on the sediment image. Its indication was caused by the influence of the boat and tow vehicle movements so that disrupt the appearance of the image (Fig. 7). The physical characteristic of the Punggur sea was having the dynamical current sea. This causes movement of the tow vehicle more difficult to control. Based on data from the movement of side scan sonar was founded the sensor pitch movements until 15 degrees from a standstill 0 degrees roll movements occur up to 10 degrees from its position as well as 0 degrees.

Image of seafloor sediments with the 7 targets. The target of 6 was the object of the sunken ship on the seafloor, while sand object can be seen clearly (Fig. 6). The ship object was founded at the coordinate of 1°03.3101N and 104°08.7362 E. On the port (right side) was seen the lighter entrenchment. Their excavation led to differences in texture, roughness and slope of the seafloor sediments. Furthermore, the excavation that occurred on the seabed was indicated causing the larger particle sediments was lifted up.

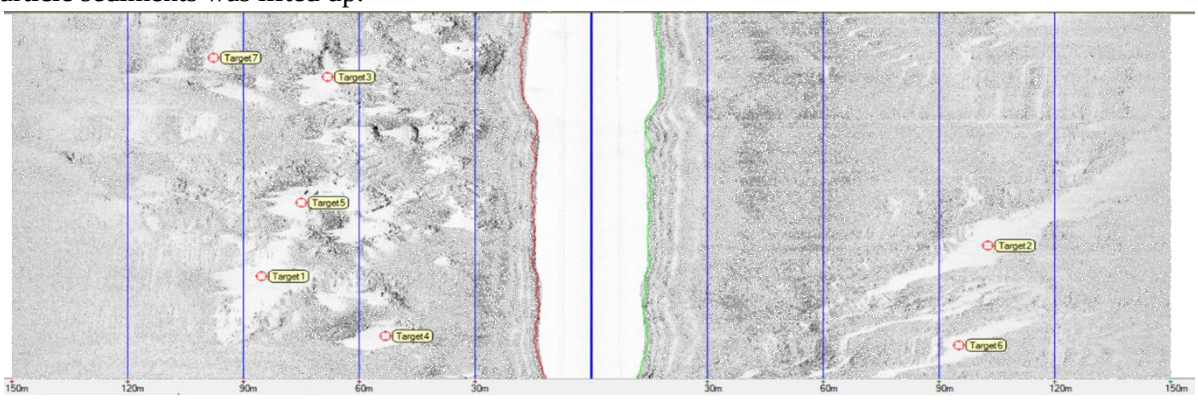

Figure 6. Image of seafloor sediments with the 7 targets

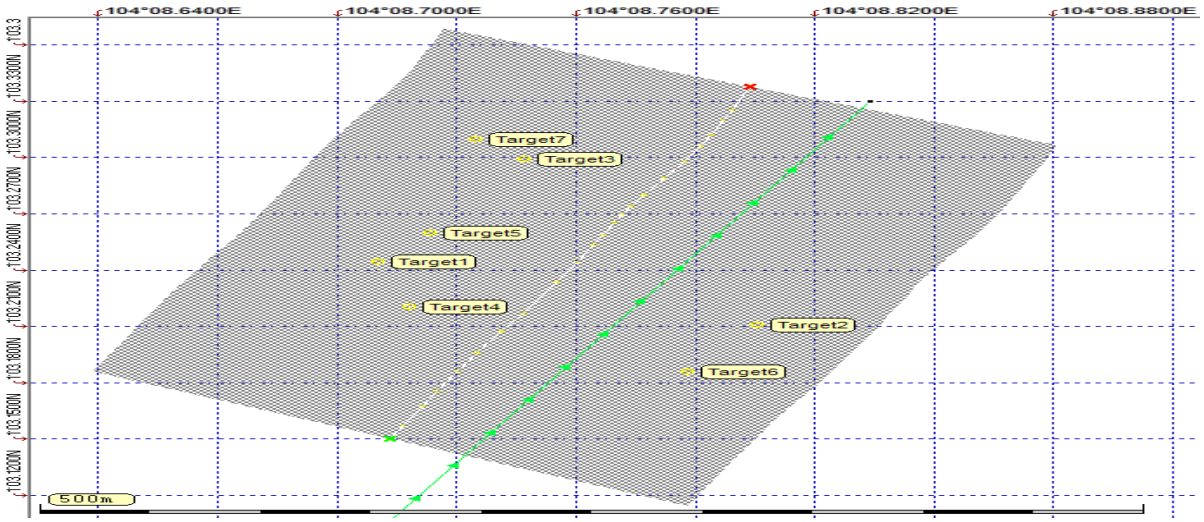

Figure 7. The target positions and the seafloor image by SSS tracking

According to [13-14] grain size, sediment surface roughness scale and significant slope variations could be important role in the acoustic response. Stated that swift currents would precipitate coarse grain sediments and the weak current would precipitate the fine-grained sediments. However, the seafloor condition will affect the location of the sediment. According to [15-16] a sweep of side scan sonar can produce mosaics, geological and sedimentology features that are easily to observe and interpreted qualitatively so could provide the information about the dynamics of the ocean floor. The beam pattern incidence angle (^{o}) of the directivity pattern (dB) and beam pattern can be seen in Figure 8.

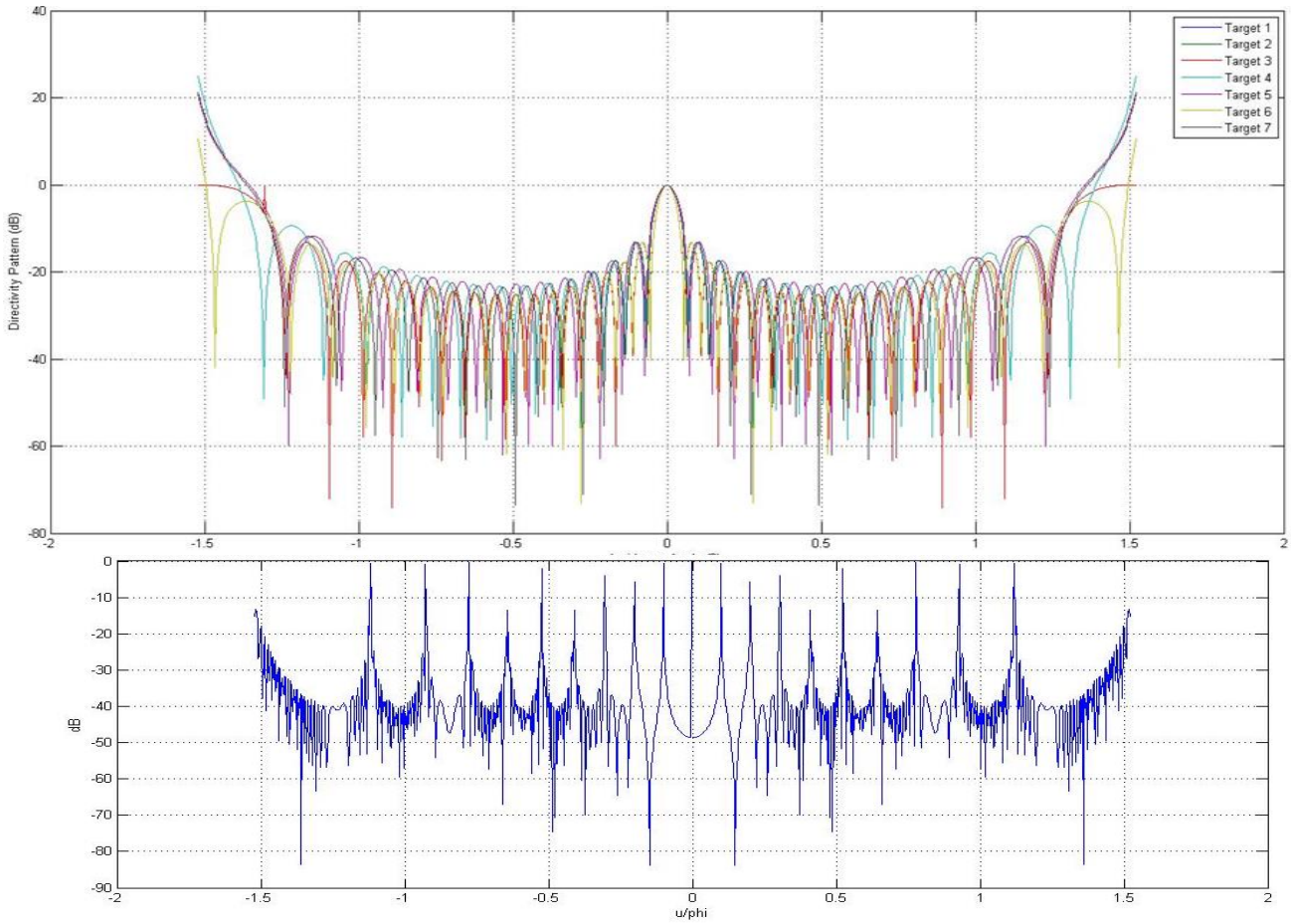

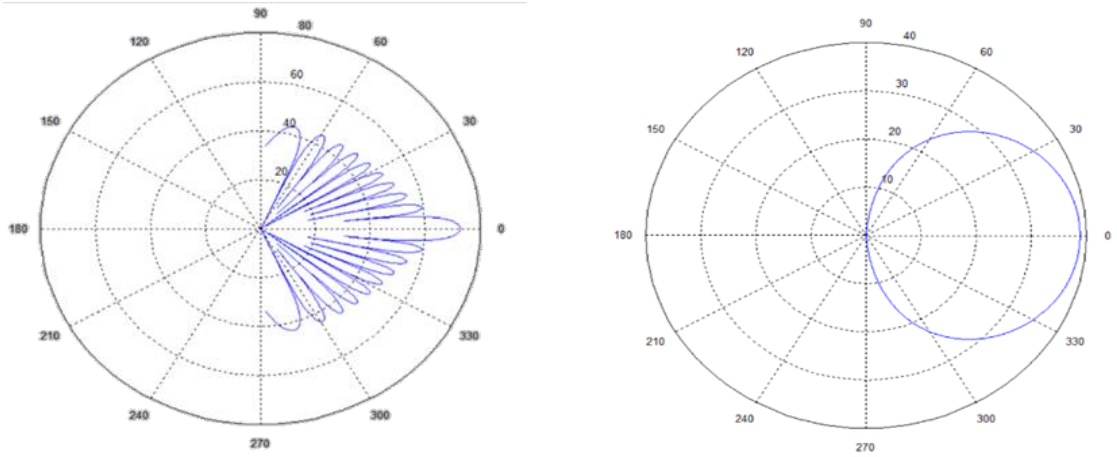

Figure 8. The beam pattern incidence angle (^{o}) of the directivity pattern (dB) and Beam pattern

The target amount as well as 7 targets on Beam pattern of Discrete-Equi-Spaced Line Array unshaded method, the target of 4 has the highest value at 21.08 dB of its directivity Pattern was shown in light blue. By looking at the center of the model beam pattern result, the target of 6 has a central value of the incidence angle (^{o}) of the directivity pattern (dB) are not in a value of 0 or at the center of the resulting beam pattern. On target of 6 there is a value of incident angle -1.5^o and 1.5^o has decreased to -40 dB. This relation can be seen to the value of altitude (m) which is 18.1m and a gain of 6 dB which allegedly was the object of the shipwreck on the seabed. On the target of 4 has the values of incident angle -1.32^o and 1.32^o and also decreased up to -50 dB. The de-convolution of this method result shows the beam pattern which was still concentrated by touching the second quadrant of the existing signal, these results provide a similar pattern the beam and a beam generated by looking at the value of the wavelength and frequency is generated [17-18]. This can be seen in relation to the value of altitude (m) which is worth 17.8 and gain value of 5 dB which is the object of the shipwreck on the seabed allegedly.

Seismic line trace of target detection have 41 number of data collection from side scan sonar imagery after processing. Highest of seismic line trace of target detection is target 3 with 1664 (Figure 9).

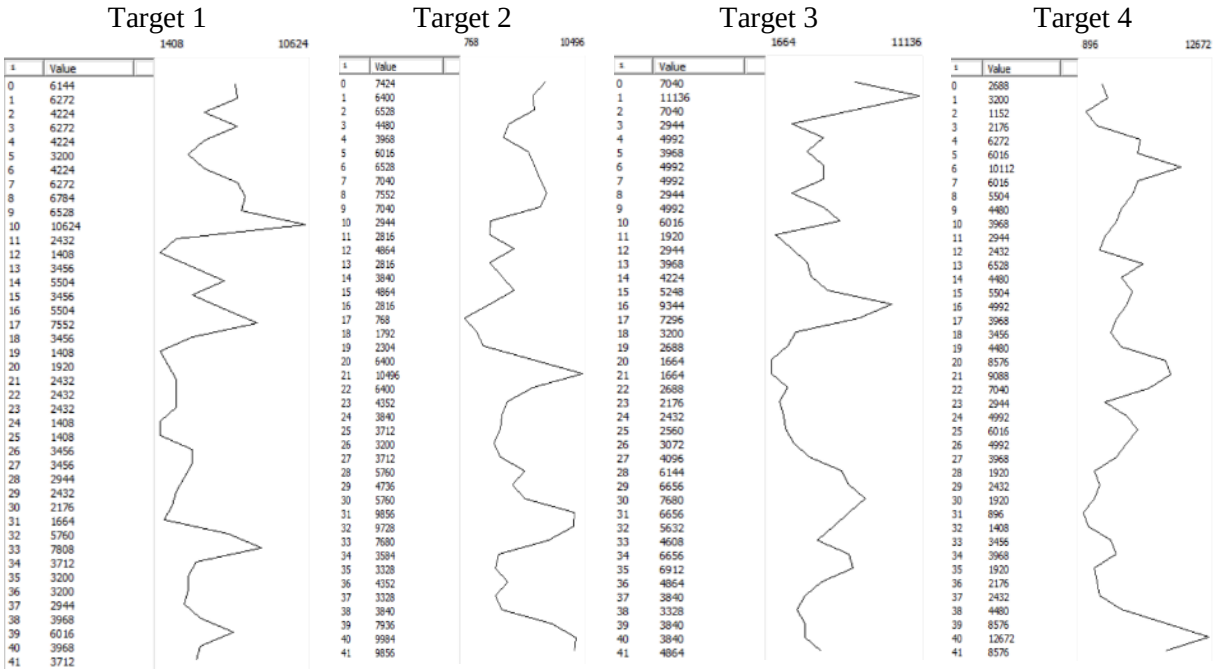

Figure 8. Seismic line trace of target detection

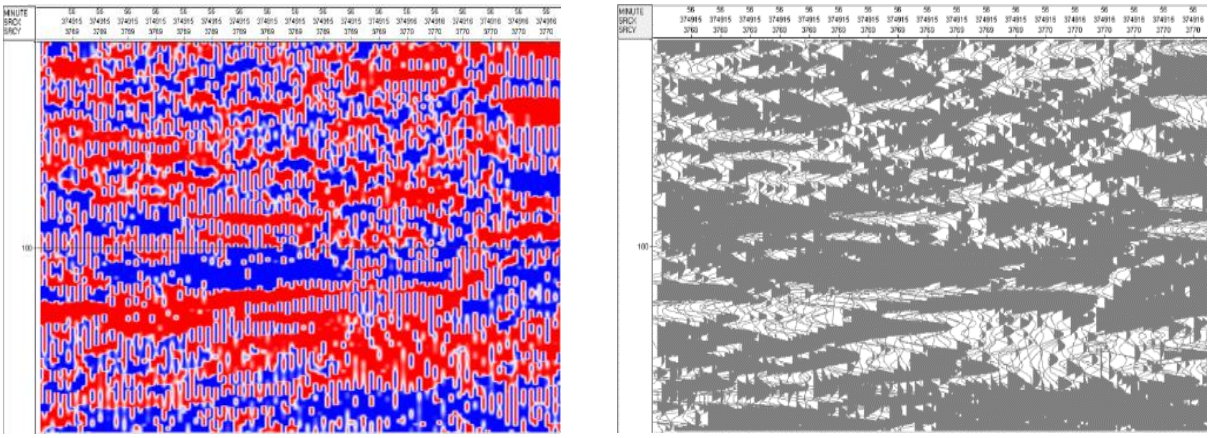

Figure 9. Seismic of Side Scan Sonar imagery

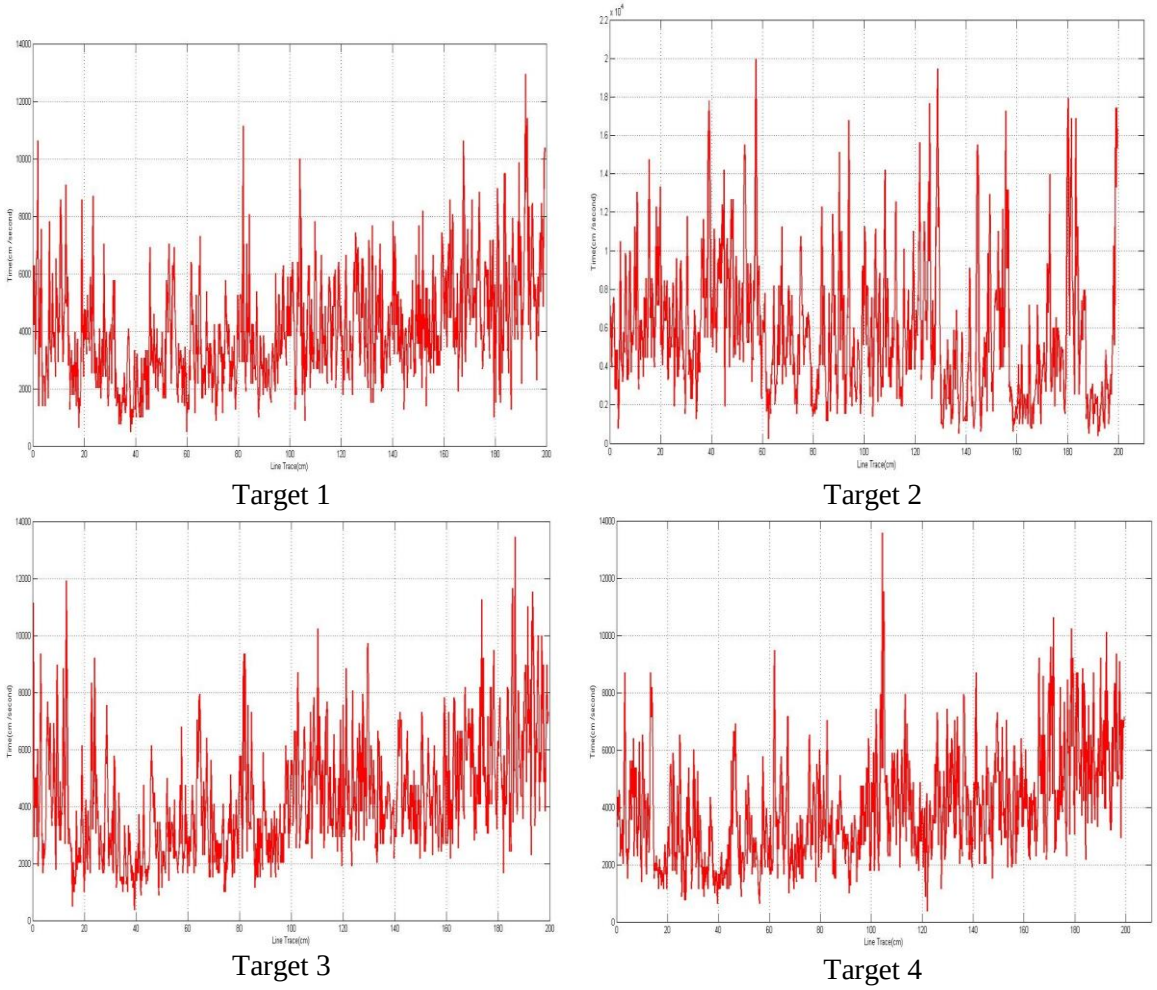

Figure 10. Line trace (cm) vs time (cm/second) target 1-4.

Identification of seismic line trace with identification target must be important for seismic investigation and analysis [19-21]. Figure of line trace vs time have max data is 200 on line trace and 220 x 103 time in target 2. Highest result of the time in Figure 9 is 12928 cm/second and 191, 88 cm

in line trace target 1 of side scan sonar imagery. Highest result of the time in figure 7 is 9968 cm/second and 57, 525 cm in line trace target 2 of side scan sonar imagery. Highest result of the time in Figure 10 is 13440 cm/second and 186, 615 cm in line trace target 3 of side scan sonar imagery. Highest result of the time in (Figure 10) is 13568 cm/second and 104, 325 cm in line trace target 4 of side scan sonar imagery. Highest result of line trace is target 1 with 191, 88 cm on target 1, and highest of time result is 13568 cm/second on target 4. Seismic figure of side scan sonar imagery have total line trace is 4479, time: 77.9547 cm/s, and gain: 0.00271091 (Figure 10).

Conclusions

The research in Punggur sea, Batam using the C-Max CM2 Side Scan Sonar Tow fish at a frequency of 325 kHz, was obtained seabed sediments more sand and found many of the target value gain and high altitude. The result of the side scan sonar (SSS) image recorded have identified seven targets, while the target of 4 and 6 based on the Discrete-Equi-Spaced unshaded Line Array method was discovered the sunken wreck. There was a perpendicular relationship between the incident angle (^{o}), directivity pattern (dB), Altitude (m), and a gain value (dB). The Discrete-Equi-Spaced unshaded Line Array was a method which can be used to identify the targets on the seabed. The highest result of the line trace was the target 1, and highest of time result on target 4. Target 1 have a relationship with results with highest target detection.

Acknowledgments

We would like to thank Batam State Polytechnic, Marine Instrument and Application Club (MIAC), and PT. Geotronix Indonesia since helped and guided us so we had finished our research.

4. References

[1] Lubis, M. Z., Anurogo, W., Khoirunnisa, H., Irawan, S., Gustin, O., & Roziqin, A. 2017. Using Side-Scan Sonar instrument to Characterize and map of seabed identification target in punggur sea of the Riau Islands, Indonesia. Journal of Geoscience, Engineering, Environment, and Technology, 2(1), 1-8.

[2] Lubis, M. Z., Lubis, R. A., & Lubis, R. U. A. 2017. Two-Dimensional Wavelet Transform De-noising and Combining with Side Scan Sonar Image. Journal Of Applied Geospatial Information, 1(01), 1-4.

[3] Bartholomä, A. 2006. Acoustic bottom detection and seabed classification in the German Bight, southern North Sea. Geo-Marine Letters, 26(3), 177.

[4] Hamilton, L. J., & Parnum, I. 2011. Acoustic seabed segmentation from direct statistical clustering of entire multibeam sonar backscatter curves. Continental Shelf Research, 31(2), 138-148.

[5] Bryant, R. S.2015. Side Scan Sonar for Hydrography-An Evaluation by the Canadian Hydrographic Service. The International Hydrographic Review, 52(1), 43-56.

[6] Wahlberg, M., Jensen, F. H., Aguilar Soto, N., Beedholm, K., Bejder, L., Oliveira, C., & Madsen, P. T. 2011. Source parameters of echolocation clicks from wild bottlenose dolphins (Tursiops aduncus and Tursiops truncatus). The Journal of the Acoustical Society of America, 130(4), 2263-2274.

[6] Frey-Martínez, J., Cartwright, J., & James, D. 2006. Frontally confined versus frontally emergent submarine landslides: a 3D seismic characterisation. Marine and Petroleum Geology, 23(5), 585-604.

[7] Alves, T. M. 2010. 3D Seismic examples of differential compaction in mass-transport deposits and their effect on post-failure strata. Marine Geology, 271(3), 212-224.

[8] Grothues, T. M., Newhall, A. E., Lynch, J. F., Vogel, K. S., & Gawarkiewicz, G. G. 2016. High-frequency side-scan sonar fish reconnaissance by autonomous underwater vehicles. Canadian Journal of Fisheries and Aquatic Sciences, 74(2), 240-255.

[9] Ruffell, A. (2014). Lacustrine flow (divers, side scan sonar, hydrogeology, water penetrating radar) used to understand the location of a drowned person. Journal of hydrology, 513, 164-168.

[10] Zhang, J., Tao, B., Liu, H., Jiang, W., Gou, Z., & Wen, F. 2016. A mosaic method based on feature matching for side scan sonar images. In Ocean Acoustics (COA), 2016 IEEE/OES China (pp. 1-6). IEEE.

[11] Powers, J., Brewer, S. K., Long, J. M., & Campbell, T. 2015. Evaluating the use of side-scan sonar for detecting freshwater mussel beds in turbid river environments. Hydrobiologia, 743(1), 127-137.

[12] Garner, J. T., Buntin, M. L., Fobian, T. B., Holifield, J. T., Tarpley, T. A., & Johnson, P. D. 2016. Use of side-scan sonar to locate Tulotoma magnifica (Conrad, 1834)(Gastropoda: viviparidae) in the Alabama River. Freshwater Mollusk Biology and Conservation, 19, 51-55.

[13] Bond, L. J., Kepler, W. F., & Frangopol, D. M. 2000. Improved assessment of mass concrete dams using acoustic travel time tomography. Part I—theory. Construction and Building Materials, 14(3), 133-146.

[14] Kenny, A. J., Cato, I., Desprez, M., Fader, G., Schüttenhelm, R. T. E., & Side, J. 2003. An overview of seabed-mapping technologies in the context of marine habitat classification☆. ICES Journal of Marine Science, 60(2), 411-418.

[15] Jain, A. D., & Makris, N. C. 2016. Maximum Likelihood Deconvolution of Beamformed Images with Signal-Dependent Speckle Fluctuations from Gaussian Random Fields: With Application to Ocean Acoustic Waveguide Remote Sensing (OAWRS). Remote Sensing, 8(9), 694.

[16] Owen, M. J., Maslin, M. A., Day, S. J., & Long, D. 2015. Testing the reliability of paper seismic record to SEGY conversion on the surface and shallow sub-surface geology of the Barra Fan (NE Atlantic Ocean). Marine and Petroleum Geology, 61, 69-81.

[17] Singh, A., Modi, M. H., Sinha, A. K., Dhawan, R., & Lodha, G. S. 2015. Study of structural and optical properties of zirconium carbide (ZrC) thin-films deposited by ion beam sputtering for soft x-ray optical applications. Surface and Coatings Technology, 272, 409-414.

[18] Zhang, Y., Wang, Y., Li, W., Huang, Y., & Yang, J. 2015. Scanning radar angular superresolution with fast standard Capon beamformer. In Geoscience and Remote Sensing Symposium (IGARSS), 2015 IEEE International (pp. 3111-3114). IEEE.

[19] Pauselli, C., Barchi, M. R., Federico, C., Magnani, M. B., & Minelli, G. 2006. The crustal structure of the northern Apennines (central Italy): An insight by the CROP03 seismic line. American Journal of Science, 306(6), 428-450.

[20] Russell, B., Hampson, D., Schuelke, J., & Quirein, J. 1997. Multiattribute seismic analysis. The Leading Edge, 16(10), 1439-1444.

[21] Lagomarsino, S., & Giovinazzi, S. 2006. Macroseismic and mechanical models for the vulnerability and damage assessment of current buildings. Bulletin of Earthquake Engineering, 4(4), 415-443.